



Robust topology optimisation of bi-modulus structures



Kun Cai^a, Qing H. Qin^{b,*}, Zhen Luo^c, Ai J. Zhang^a

^a College of Water Resources and Architectural Engineering, Northwest A&F University, Yangling 712100, China

^b College of Engineering and Computer Science, The Australia National University, Canberra, Australia

^c School of Electrical, Mechanical and Mechatronic Systems, The University of Technology, Sydney, Australia

HIGHLIGHTS

- Robust topology optimisation of bi-modulus material is developed.
- Multiple loading conditions are considered in simulation.
- Material replacement method is adopted for simplifying structural analysis.
- Sensitivity of robust compliance is derived.
- Optimal topology is found to be force-direction dependent when materials display bi-modulus behaviour.

ARTICLE INFO

Article history:

Received 11 January 2013

Accepted 7 May 2013

Keywords:

Robust design

Topology optimisation

Bi-modulus

Multi-stiffness structures

ABSTRACT

This study proposes a robust topology optimisation method for the design of bi-modulus structures under uncertain multiple loading conditions (MLC). The objective of the design optimisation is to minimise the standard deviation of the weighted structural compliance. The gradient-based method is applied to perform a sensitivity analysis for the identification of optimal design variables. A material replacement method is used to overcome difficulty in the sensitivity analysis due to the stress-dependent behaviour of the original bi-modulus material. In the material replacement operation, two new isotropic materials are identified to replace the original bi-modulus material according to its two moduli. To reduce the side effects of the material replacement operation on the final design, the local stiffness is modified in terms of the stress state. Typical numerical examples are used to demonstrate the effectiveness of the proposed method to the final design, including the load uncertainty on the optimal bi-modulus layout, as well as other factors, such as loading direction and the ratio between the two moduli of the bi-modulus material. The comparison between layouts of isotropic and bi-modulus materials also shows that the final bi-modulus material distribution is sensitive to loading directions in practical designs.

© 2013 Elsevier Ltd. All rights reserved.

1. Introduction

Topology optimisation is a powerful computational tool for the conceptual design stage of structural optimisation. Optimising the topology of a structure is highly challenging because it is required to automatically determine an optimal material layout in the design domain. Topology optimisation has undergone considerable development over the past two decades with a variety of applications [1]. Topology optimisation can essentially be regarded as a numerical procedure to iteratively re-distribute a given amount of material to optimise a prescribed objective function under specific constraints in a reference domain subject to supports and

loads. Thus far the typical topological optimisation methods include the ground structure-based method [2], the homogenisation-based method [3], the SIMP method (solid isotropic material with penalisation) [4,5], the ESO (evolutionary structural optimisation) method [6–8], and the level set method, which has emerged recently [9–11].

There are a number of uncertainties in the design of structures, including the operating environment, which can be modelled using various methods [12] such as the reliability-based optimisation (RBO) [13,14] and the robust design optimisation (RDO) methods [15–17]. In engineering, variations as a result of uncertainties can lead to significant performance changes for the structural system. Thus, there is increasing demand to quantitatively consider the impact of uncertainties in the optimisation to ensure safety and to avoid the breakage and collapse of structural systems under extreme working conditions.

In topology optimisation, uncertain variations of structural parameters, material properties and external loads will have

* Corresponding author. Tel.: +61 261258274.

E-mail addresses: kuicansj@sohu.com (K. Cai), qinghua.qin@anu.edu.au (Q.H. Qin), zhen.luo@uts.edu.au (Z. Luo), Zaj@nwsuaf.edu.cn (A.J. Zhang).

considerable effects on optimised structural performance. The uncertain parameters are primarily taken into account in the optimisation to establish robust and reliability-based topological designs. There have been a large number of researchers who have focused their study on reliability-based topology optimisation problems. For instance, Kharmanda and Olhoff [18] studied a reliability-based topology optimisation (RBTO) method to seek the optimal structural layout by satisfying probabilistic constraints, which considered the topology optimisation of continuum structures with stochastic distribution of the material elastic modulus, geometrical thickness and externally applied loads [19]. Probabilistic reliability constraints were also considered in the topology optimisation of micro mechanical systems (e.g., [20–22]). Jung and Cho [23] proposed a reliability-based method for the topology optimisation of geometrically nonlinear structures. Luo et al. [24] proposed a non-probabilistic reliability topology optimisation method using ellipsoid convex models. Guest and Igusa [25] proposed a structural topology optimisation method that considered uncertainty loads (both in the magnitude and location) and small uncertainty in the nodal location. Silva et al. [26] investigated the reliability topology optimisation of structures under component and system reliabilities. Nguyen et al. [27] presented a single-loop System Reliability-based Topology Optimisation method, accounting for the statistical dependence of multiple limit-states.

Robustness has also recently been considered in topology optimisation problems. Kang and Luo [28] provided a geometrically nonlinear structural topology optimisation with non-probabilistic reliability. Chen et al. [29] investigated a level-set based robust topological shape optimisation method considering random field uncertainties in loading and material properties. Kogiso et al. [30] discussed a robust topology optimisation method for compliant mechanisms under uncertain external loading. Seepersad et al. [31] proposed a robust topology optimisation method for evaluating the impact of dimensional tolerances and topological imperfections. The imperfections deviate from the intended prismatic cellular structure and customised elastic material properties with local Taylor-series approximations. In addition to the reliability and robust topology optimisation, Luo et al. [32] proposed an uncertain topology optimisation method for multi-stiffness structures using a fuzzy set theory to account for the uncertainty of the system.

It can be observed that most current topology optimisation problems, especially topology designs under uncertain conditions, are based on isotropic material models, which are applicable in most cases for a wide range of practical designs. However, there exists a large family of structures with bi-modulus materials that are popular in many engineering designs, e.g., concrete, plastic, synthetic rubber, cast iron, etc. Such materials exhibit different behaviours along the same direction, i.e., the tension modulus is different from the compression module. For the design of bi-modulus structures, most conventional topology optimisation methods may not be computationally effective because the mechanical behaviour of bi-modulus materials is stress-dependent. Briefly, the principal directions of a bi-modulus material align with the local stress state; this means that they align with the principal directions of the stress tensor. For common orthotropic material, the material principal directions are fixed and the difference between the moduli occurs between different directions. Due to the nonlinearity of mechanical properties of bi-modulus structures [33–35], iterative re-analysis of structures is required for accurately evaluating the stress field of bi-modulus structures, which will lead to several repetitions of numerical analysis to find the accurate displacement solutions before updating the design variables at every loop.

There are only a very limited number of research studies concerned with topology optimisation of structures with bi-modulus materials [36–41] or bi-strength materials [42–45], and most of the previous investigations have not considered uncertainty in

their designs [7,8,36–45]. Although RDO has been widely studied in a border range of design applications [16], it has not been applied to topology optimisation of bi-modulus structures due to the difficulty of sensitivity analysis for updating design variables via gradient-based approaches. Meanwhile, in a practical design, a structure is primarily subjected to multiple loading cases (MLC) [32,46–48]. Hence, this study aims to present a new robust topology optimisation method for the design of bi-modulus structures under multiple uncertain loading cases and to investigate the effects of load directions on material layout.

It is noted that there are two categories of methods of structure topology optimisation: the first is the stiffness design that aims to minimise the structural mean compliance subject to an overall volume constraint (e.g., [1,3,4,9–11,41]), and the second is the strength design that aims to minimise the weight of the structure subject to local stress constraints (e.g., [42–45,49,50]). These are two methodologies for topology optimisation of structures from two different aspects of structural stiffness and strength design philosophies. However, this research mainly focuses on topology optimisation problems in the context of structural stiffness design.

2. Methodology

2.1. Formulation of robust optimisation

2.1.1. General probability model

Generally, the characters of most random uncertainties can be represented using appropriate probability models. In the probability model frame, uncertainty is expressed in terms of random variables or a random field that conforms to a specified distribution, such as a normal or Gaussian distribution. At the same time, the target function will be expressed as a random variable or random field. In this study, probability analysis is adopted to estimate the distribution of the target function. For example, assuming that $\mathbf{s} = [s_1, s_2, \dots, s_M]^T$ is formulated with independent random variables that conform to a Gaussian distribution (marked with $N(\cdot)$),

$$s_i \sim N(\bar{s}_i, \sigma_i^2(s_i)), \quad i = 1, 2, \dots, M \quad (1)$$

where \bar{s}_i and σ_i are the expectation (or mean value) and the standard deviation of s_i , respectively. The target function can be expressed as a random variable according to a Gaussian distribution, shown as follows:

$$f(\mathbf{s}) \sim N(\bar{f}, \sigma^2(f)) \quad (2)$$

where \bar{f} and $\sigma(f)$ are the expected value and the standard deviation of f , respectively. Commonly, numerical methods such as the Monte Carlo method can be used to search the parameters of the target function; however, the computational cost is excessive for topology design problems. Therefore, in the present study, a random FEM method is adopted to calculate the parameters of the target function.

2.1.2. Equivalent elasticity of bi-modulus material

The elasticity of a bi-modulus material is stress-dependent, as a bi-modulus material has a tension modulus E_T and compression modulus E_C . For convenience, the ratio between E_T and E_C is defined as:

$$R_{TCE} = \frac{E_T}{E_C}. \quad (3)$$

Clearly, the bi-modulus material is considered to be purely isotropic if $R_{TCE} = 1$.

Table 1 shows equivalent elasticity models of a bi-modulus unit volume under plane stress/strain states. As a material under pure compression or pure tension, the bi-modulus material exhibits

Table 1
Mechanical behaviour of bi-modulus material under different plane stress states.

Stress state	Bi-modulus material	True elasticity
Pure tension		
Pure compression		
Complex state		

σ_1 the first principal stress, σ_3 the third principal stress, $\sigma_1 \geq \sigma_3$.

isotropic behaviour. Under complicated stress states, however, the elasticity of the bi-modulus material is orthotropic (strictly, transversely isotropic) and the principal material directions align with the principal stress directions. Structural re-analysis is required due to the material's bi-modulus behaviour. The accurate deformation of continua with bi-modulus material can be obtained using structural re-analysis [33,34]. In re-analysis, both the elastic matrix and the principal directions of the material are required to change.

Double loops are generally part of structural topology optimisations. The inner loop is for structural analysis and the outer loop is for the update of design variables, increasing the duration of time required for numerical computation. We can observe in Table 1 that the material exhibits isotropic behaviour under pure tension or pure compression. As isotropic material is not stress-dependent; replacing the original bi-modulus material with an isotropic material can avoid the inner loop in the optimisation. However, the local stiffness should be adjusted, as the local stress state is complex. The adjustment scheme is described in Section 2.4.

2.1.3. Optimisation model under deterministic loads

As mentioned, topological design problems of structures can be formulated from two different aspects: the stiffness design and the strength design. This study focuses on stiffness design to

minimise the structural mean compliance under a global volume constraint. Hence, in the context of structural stiffness design, the topology optimisation problem can be established as follows under deterministic multiple loading cases: [1]

$$\begin{aligned}
 &\text{Find } \{\rho_m\} \text{ on } \Omega \\
 &\min c_w = \sum_{l=1}^{N_{LC}} w_l \bar{c}_l \\
 &\text{s.t. } \sum_m v_m \rho_m - f_v \cdot V_0 = 0 \\
 &K_l \cdot U_l = P_l, \quad (l = 1, 2, \dots, N_{LC}) \\
 &\rho_m \in [\rho_{\min} \quad 1.0]
 \end{aligned} \tag{4}$$

where the design variables ρ_m are the relative densities of elements in the design domain. The objective function, c_w , is structural total compliance under MLC; w_l is the pre-defined positive weighting coefficient; $c_l = P_l^T \cdot U_l$ is structural compliance under the l -th loading condition; \bar{c}_l is the modified value of structural compliance (c_l) with new isotropic materials replacing the original bi-modulus material; K_l is the global stiffness matrix of a structure under the l -th loading condition, which are determined using well-established finite element method [51,52]; and U_l and P_l are the global nodal displacement vector and nodal force vector, respectively. K_l and P_l can be calculated using the finite element approach. $\rho_{\min} = 0.001$ is used to avoid singularity of K_l .

2.1.4. Optimisation model under uncertain loads

If the magnitudes of loads or material parameters are uncertain, the stiffness design of the structure becomes complex. According to the principle of robust design optimisation [53], i.e., to select reasonable design variables in reducing the sensitivity of objective function to the uncertainties, in robust stiffness design, the objective function is not to find a structure with minimum expected compliance (using RBO) but to identify a structure whose compliance varies with uncertain loads as little as possible within the feasible space.

In the present study, the uncertainties are assumed to be the external load applied on the structure only, and we present a RDO method to solve the continuum topology optimisation under MLC. This means that, in the conceptual design phase, the uncertainty of loads is considered to give the optimal material layout to idealise the structure's reliability and stability. In this study, for the sake of simplicity, only an overall volume constraint is considered in the RDO formulation.

Under uncertain loads, the volume-constrained robust stiffness design of a continuum with bi-modulus material under weighted MLC is defined as follows:

$$\begin{aligned} & \text{Find } \{\rho_m\} \text{ on } \Omega \\ & \min \sigma\{c_w\} = \sigma \left\{ \sum_{l=1}^{N_{LC}} w_l \bar{c}_l \right\} \\ & \text{s.t. } \sum_m v_m \rho_m - f_v \cdot V_0 = 0 \\ & K_l(\{\rho_m\}) \cdot U_l(\{\rho_m\}, \mathbf{p}_l) = P_l(\mathbf{p}_l), \\ & \quad (l = 1, 2, \dots, N_{LC}) \\ & \quad \rho_m \in [\rho_{\min} \quad 1.0] \end{aligned} \quad (5)$$

where $\sigma\{c_w\}$ is the standard deviation of weighted structural compliance under MLC; $\mathbf{p}_l = [p_{l,1}, p_{l,2}, \dots, p_{l,n(l)}]^T$ is the vector with uncertain parameters of the l -th load as components, and each variable has a Gaussian distribution; $n(l)$ is the number of uncertain parameters of the l -th load; and \bar{c}_l is the modified structural compliance ($c_l = P_l^T \cdot U_l$) under the l -th loading.

To use the mathematical programming method for solving the optimisation problem, the binary design with discrete variables of 0 and 1 is generally relaxed and intermediate values from 0 to 1 are considered as a continuous design, i.e., $\rho_m \in [\rho_{\min} \quad 1.0]$. However, the amount of mid-density elements should be reduced. The power-law rule [5] is commonly adopted to manage this difficulty. Using this rule, the elastic matrix of porous material with the relative density of ρ_m can be expressed as follows:

$$D_{m,\rho} = \rho_m^p \cdot D_{m,s} \quad (6)$$

where the subscript "S" in $D_{m,s}$ means solid element.

2.2. Strain energy densities (SED)

In numerical simulation, the material in each element exhibits isotropic behaviour even under complicated stress states after the material replacement operation has been completed. The SED of each element is calculated for each iteration to select the modulus of the material and to consider the bi-modulus behaviour of the original material.

Here, we define the average tension SED and compression SED of an element (e.g., the m -th element) as follows:

(a) Tension SED

$$\begin{aligned} \text{TSED}_m &= \frac{1}{2N_G} \sum_{l=1}^{N_{LC}} \sum_{\text{Gaus}=1}^{N_G} \sum_{j=1}^3 \frac{w_l}{2} \\ &\quad \times (\sigma_{j,\text{Gaus},l} + |\sigma_{j,\text{Gaus},l}|) \cdot \varepsilon_{j,\text{Gaus},l} \end{aligned} \quad (7)$$

where N_G is the number of Gauss integration points of element and $\sigma_{j,\text{Gaus},l}$ and $\varepsilon_{j,\text{Gaus},l}$ are the j -th principal stress and strain of the Gauss-th integration point under the l -th loading case, respectively. This formula implies that only non-negative principal stresses contribute to the tension SED.

(b) Compression SED is defined as follows:

$$\begin{aligned} \text{CSED}_m &= \frac{1}{2N_G} \sum_{l=1}^{N_{LC}} \sum_{\text{Gaus}=1}^{N_G} \sum_{j=1}^3 \frac{w_l}{2} \\ &\quad \times (\sigma_{j,\text{Gaus},l} - |\sigma_{j,\text{Gaus},l}|) \cdot \varepsilon_{j,\text{Gaus},l} \end{aligned} \quad (8)$$

This formula implies that only non-positive principal stresses contribute to the compression SED.

Therefore, the current total SED of the element is given as follows:

$$\text{SED}_m = \text{TSED}_m + \text{CSED}_m. \quad (9)$$

However, the SED in Eq. (9) is the total SED of the element with replacement (isotropic) material. If the stress state is simple, the values of SED either with bi-modulus material or isotropic replacement material should be equal. As the element under a complex stress state, the local SED of an element with the original bi-modulus material should be different from the value given according to Eq. (9). We can therefore define the effective SED of an element, which is a modification of the SED in Eq. (9), for a complex stress state as follows:

$$\begin{aligned} \text{SED}_m^{\text{effective}} &= \frac{1}{2N_G} \sum_{l=1}^{N_{LC}} \sum_{\text{Gaus}=1}^{N_G} \sum_{j=1}^3 w_l \\ &\quad \times (\text{sign}(\sigma_{j,\text{Gaus},l}) \cdot \sigma_{j,\text{Gaus},l} \cdot \varepsilon_{j,\text{Gaus},l}). \end{aligned} \quad (10)$$

The value of $\text{sign}(\cdot)$ in the above equation is determined by the current material modulus and the stress state, which can be described as follows:

(a) If the "current" material modulus of an element is E_T , then we have

$$\text{sign}(\sigma_j) = \begin{cases} 1 & \text{for } \sigma_j \geq 0 \\ R_{TCE} & \text{for } \sigma_j < 0. \end{cases} \quad (11)$$

This means that only when the principal stress is negative and the current modulus is E_T , the value of the principal stress must be modified to keep the local deformation (principal strains) the same before and after the material replacement operation.

(b) If the "current" material modulus of an element is E_C , then we have

$$\text{sign}(\sigma_j) = \begin{cases} 1 & \text{for } \sigma_j \leq 0 \\ R_{TCE}^{-1} & \text{for } \sigma_j > 0. \end{cases} \quad (12)$$

If the stress state is simple, namely, under a pure tension or a pure compression state, the effective value of SED in Eq. (10) will be equal to that of SED in Eq. (9).

2.3. Modification factor of local stiffness

Eqs. (9) and (10) may lead to different values of SED with respect to the tension or compression stress. To consider the difference in local stiffness caused by material replacement, the amount of local material should be adjusted before updating the design variable of an element. Using the current total SED and the effective SED, the modification factor of the local (m -th element) stiffness can be evaluated according to the following equation:

$$f_m = \max \left(10^{-6}, \frac{\text{SED}_m^{\text{effective}}}{\max(10^{-30}, \text{SED}_m)} \right). \quad (13)$$

Eqs. (9) and (10) show that the value of $SED_m^{\text{effective}}$ must be no higher than SED_m . Since the value of SED_m is very low, less than 10^{-30} , the m -th element has no contribution to the stiffness of the structure and can therefore be neglected. The value of f_m , less than the ratio of $SED_m^{\text{effective}}$ on SED_m , has a slight effect on the updated density of the m -th element.

2.4. Update of modulus of replacement (isotropic) material

Eqs. (9) and (10) present the effects of tension stress(es) and compression stress(es) on local stiffness. Intuitively, to approximate the original bi-modulus behaviour of an element, the local material behaviour of the element should be determined by whichever value is greater between TSED and CSED. The modulus of local material should be E_T if the tension SED is greater than compression SED, and vice versa. The selection can be expressed as follows:

$$E_m = \begin{cases} E_T, & \text{for TSED}_m > \text{CSED}_m \\ E_C, & \text{for TSED}_m < \text{CSED}_m \\ \max(E_T, E_C), & \text{others.} \end{cases} \quad (14)$$

2.5. Sensitivity analysis of objective function

To solve the optimisation problem in Eq. (5) effectively, the gradient-based programming method is adopted to update the design variables. Below is the sensitivity analysis.

For the l -th loading condition, the mean structural compliance is

$$c_l = U_l^T \cdot P_l = \left(\sum_{m=1}^{N_{El}} u_m^T \cdot k_m \cdot u_m \right)_l \quad (15)$$

and the modified mean structural compliance is the following:

$$\bar{c}_l = M_l \cdot P_l^T \cdot U_l = \left(\sum_{m=1}^{N_{El}} u_m^T \cdot (f_m \cdot k_m) \cdot u_m \right)_l \quad (16)$$

where M_l is the modification function of f_m in the l -th load case; N_{El} is the total number of elements in the structure; and u_m is the nodal displacement vector of the m -th element with stiffness matrix k_m . f_m is the modification factor of the m -th element due to material replacement and is given in Eq. (13).

As the loads are deterministic, the sensitivity of the objective function can be expressed as

$$\begin{aligned} \frac{\partial c_w}{\partial \rho_m} &= \frac{\partial}{\partial \rho_m} \left\{ \sum_{l=1}^{N_{LC}} w_l M_l \cdot P_l^T \cdot U_l \right\} \\ &= \sum_{l=1}^{N_{LC}} w_l M_l \cdot \frac{\partial (P_l^T \cdot U_l)}{\partial \rho_m} \\ &= \sum_{l=1}^{N_{LC}} w_l M_l \cdot \left(-U_l^T \cdot \frac{\partial K_l}{\partial \rho_m} \cdot U_l \right) \\ &= -\frac{f_m p}{\rho_m} \cdot \sum_{l=1}^{N_{LC}} w_l \cdot (u_m^T \cdot k_m \cdot u_m)_l \end{aligned} \quad (17)$$

where u_m represents the nodal displacement vector of the m -th element.

As the loads show uncertainty, the Rosenblatt transformation [54] is adopted to transform them into a set of uncorrelated normal variables. The first order Taylor series expansion of structural compliance at mean values of uncertain loads (normalised) is

calculated as follows:

$$c_w = c_w(\{\rho_m\}, \{\bar{p}_{li}\}) + \sum_{l=1}^{N_{LC}} \sum_{i=1}^{F(l)} \frac{\partial (w_l \bar{c}_l)}{\partial p_{l,i}} \Big|_{\bar{p}_{l,i}} (p_{l,i} - \bar{p}_{l,i}) \quad (18)$$

where $p_{l,i}$ is the i -th uncertain force under the l -th loading case. $\bar{p}_{l,i}$ is the mean value of $p_{l,i}$. $F(l)$ is the total number of uncertain forces under the l -th loading condition.

Under each loading condition, the partial differentiation of the discretised equilibrium equation of the structure is given as follows:

$$\frac{\partial (K_l \cdot U_l)}{\partial p_{l,i}} = \frac{\partial P_l}{\partial p_{l,i}}, \quad \begin{matrix} (l = 1, 2, \dots, N_{LC}) \\ (i = 1, 2, \dots, F(l)) \end{matrix} \quad (19)$$

where $F(l)$ represents the number of uncertain forces in the l -th loading condition.

As the global stiffness matrix is not relevant to loading, for each loading condition, the following discretised function is sufficient:

$$K_l \cdot \frac{\partial U_l}{\partial p_{l,i}} = \frac{\partial P_l}{\partial p_{l,i}}, \quad \begin{matrix} (l = 1, 2, \dots, N_{LC}) \\ (i = 1, 2, \dots, F(l)) \end{matrix}. \quad (20)$$

Using Eq. (20) in Eq. (18) leads to the following:

$$\begin{aligned} c_w &= c_w(\{\rho_m\}, \{\bar{p}_{li}\}) + 2 \sum_{l=1}^{N_{LC}} \sum_{i=1}^{F(l)} \left[\frac{\partial (w_l \cdot M_l \cdot P_l)}{\partial p_{l,i}} \cdot U_l \right]_{\bar{p}_{l,i}} \\ &\quad \times (p_{l,i} - \bar{p}_{l,i}). \end{aligned} \quad (21)$$

Here, the unit virtual load vector is defined as follows:

$$\delta P_{l,i} = \frac{\partial P_l}{\partial p_{l,i}}. \quad (22)$$

Therefore, the objective function, a form of the standard deviation of the weighted compliance of the structure, is expressed as follows:

$$\begin{aligned} \sigma\{c_w\} &= 2 \sqrt{\sum_{l=1}^{N_{LC}} \sum_{i=1}^{F(l)} (w_l \cdot M_l \cdot \delta P_{l,i} \cdot U_l)_{\bar{p}_{l,i}}^2 \sigma_{p_{l,i}}^2} \\ &= 2 \sqrt{\sum_{l=1}^{N_{LC}} \sum_{i=1}^{F(l)} \sum_{e=1}^{N_{El}} (w_l \cdot f_e \cdot (\delta u_{l,i}^e)^T \cdot k_e \cdot u_l^e)_{\bar{p}_{l,i}}^2 \sigma_{p_{l,i}}^2} \\ &= 2 \sqrt{\sum_{l=1}^{N_{LC}} \sum_{i=1}^{F(l)} \sum_{e=1}^{N_{El}} (w_l \cdot f_e \cdot \delta \Pi_{l,i}^e)_{\bar{p}_{l,i}}^2 \sigma_{p_{l,i}}^2} \end{aligned} \quad (23)$$

where f_e is the modification factor of the e -th element; k_e is the stiffness matrix of the e -th element; $\delta u_{l,i}^e$ is the nodal virtual displacement vector of the element with respect to the virtual load; $\delta P_{l,i}$, u_l^e is the nodal true displacement vector of the element under the l -th loading condition; and $\sigma_{p_{l,i}}$ is the standard deviation of $p_{l,i}$.

For the equilibrium state, the following equation is sufficient:

$$\frac{\partial (K_l \cdot U_l)}{\partial \rho_m} = \frac{\partial K_l}{\partial \rho_m} \cdot U_l + K_l \frac{\partial U_l}{\partial \rho_m} = \frac{\partial P_l}{\partial \rho_m} = 0. \quad (24)$$

Hence,

$$\frac{\partial U_l}{\partial \rho_m} = -K_l^{-1} \frac{\partial K_l}{\partial \rho_m} \cdot U_l. \quad (25)$$

According to Eqs. (24) and (25), we can obtain the following equation:

$$\begin{aligned} \frac{\partial (\delta P_{l,i}^T \cdot U_l)}{\partial \rho_m} &= -(\delta P_{l,i}^T \cdot K_l^{-1}) \frac{\partial K_l}{\partial \rho_m} \cdot U_l \\ &= -\delta U_{l,i}^T \frac{\partial K_l}{\partial \rho_m} \cdot U_l. \end{aligned} \quad (26)$$

It is necessary to mention that the additional loading conditions with respect to $\delta P_{l,i}$ should be considered to efficiently obtain the sensitivity of the objective function.

At the mean value of the load, $\bar{p}_{l,i}$, Eq. (26) can be expressed as follows:

$$\begin{aligned} \frac{\partial (\delta P_{l,i}^T \cdot U_l)}{\partial \rho_m} \Big|_{\bar{p}_{l,i}} &= - \left[\sum_{e=1}^{N_{EL}} (\delta u_e)^T \cdot \frac{\partial k_e}{\partial \rho_m} \cdot u_e \right]_{\bar{p}_{l,i}} \\ &= - \frac{p}{\rho_m} [(\delta u_m)^T \cdot k_m \cdot u_m]_{\bar{p}_{l,i}} \\ &= - \frac{p}{\rho_m} \delta \Pi_m \Big|_{\bar{p}_{l,i}}. \end{aligned} \tag{27}$$

Therefore, the sensitivity of the objective function is expressed as follows:

$$\begin{aligned} \frac{\partial \sigma \{c_w\}}{\partial \rho_m} &= \frac{1}{\sigma \{c_w\}} \frac{\partial}{\partial \rho_m} \\ &\times \left\{ \sum_{l=1}^{N_{LC}} \sum_{i=1}^{F(l)} [(w_l M_l \cdot \delta P_{l,i}^T) \cdot U_l]_{\bar{p}_{l,i}}^2 \sigma_{p_{l,i}}^2 \right\} \\ &= \frac{2}{\sigma \{c_w\}} \left\{ \sum_{l=1}^{N_{LC}} \sum_{i=1}^{F(l)} \left[\sum_{m=1}^{N_{EL}} w_l f_m \cdot \delta \Pi_m \right] \right. \\ &\quad \left. \cdot \frac{-p w_l \cdot f_m \cdot \delta \Pi_m}{\rho_m} \Big|_{\bar{p}_{l,i}} \sigma_{p_{l,i}}^2 \right\} \\ &= \frac{-2p \cdot f_m}{\sigma \{c_w\} \cdot \rho_m} \left\{ \sum_{l=1}^{N_{LC}} w_l^2 \cdot \sum_{i=1}^{F(l)} \left[\left(\sum_{e=1}^{N_{EL}} f_e \cdot \delta \Pi_e \right) \right. \right. \\ &\quad \left. \left. \cdot \delta \Pi_m \right]_{\bar{p}_{l,i}} \sigma_{p_{l,i}}^2 \right\}. \end{aligned} \tag{28}$$

2.6. Update of design variables

The optimal criterion (OC) method [1] is adopted to update the design variables. For the m -th element at the k -th step, the update scheme is given as follows:

$$\rho_m^{(k+1)} = \begin{cases} \max \{ \rho_{\min}, \rho_m^{(k)} - \delta \} & \text{for } \rho_m^{(k)} L_m \leq \max \{ \rho_{\min}, \rho_m^{(k)} - \delta \} \\ \rho_m^{(k)} L_m & \text{others} \\ \min \{ 1.0, \rho_m^{(k)} + \delta \} & \text{for } \rho_m^{(k)} L_m \geq \min \{ 1.0, \rho_m^{(k)} + \delta \} \end{cases} \tag{29}$$

where δ , or the maximum incremental of relative density, is 0.1 for this study. L_m can be calculated according to the following equation:

$$L_m = \sqrt{\left| \frac{\partial \sigma \{c_w\}}{\partial \rho_m^{(k)}} \right| / \left(\lambda \frac{\partial V_m}{\partial \rho_m^{(k)}} \right)} \tag{30}$$

where the popular bi-sectioning algorithm [55] is used to obtain the value of the Lagrangian multiplier λ in Eq. (30). It should be noted that the above equation involves a square root that is always positive. More details regarding the above equation can be found in the report by Sigmund [55]. Several methods can be used to eliminate the numerical instabilities in the SIMP-based topology optimisation problems, such as sensitivity and density filtering schemes [55,56]. In this study, the standard sensitivity filter is included to avoid chequerboard patterns in the topological design [55].

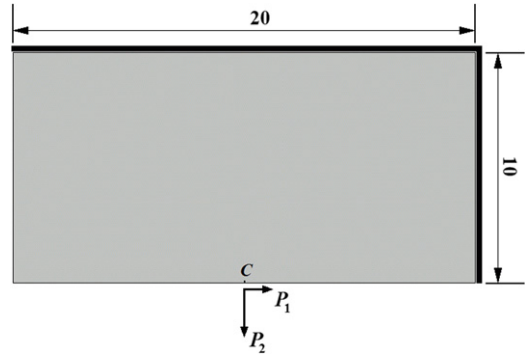


Fig. 1. Design domain.

2.7. Flow chart of the optimisation algorithm

- Step 1: Create the FE model of structure and give an initial design, let $k = 1$;
- Step 2: Analyse structural deformation and obtain stress and strain fields of all of the loading conditions (in total, $N_{LC} + \sum_{l=1}^{N_{LC}} F(l)$);
- Step 3: Calculate TSED, CSED, total SED and effective SED of each element (Eqs. (7)–(10));
- Step 4: Calculate modification factor of each element (Eq. (13));
- Step 5: Select the modulus of replacement material of each element (Eq. (14));
- Step 6: Calculate objective function, sensitivities of objective function and constraint function(s) (Eq. (28));
- Step 7: Update design variables (Eq. (29));
- Step 8: $k = k + 1$; If Eq. (31) is satisfied or $k > 50$, then go to Step 9; else go to Step 2;
- Step 9: Stop.

The termination criterion in Step 8 is given as follows:

$$\left| \frac{c_{w,k} - c_{w,j}}{c_{w,k}} \right| \leq \eta, \quad 1 < j = k - n, k - n + 1, \dots, k - 1 \tag{31}$$

where the algorithm tolerance is $\eta = 0.001$ and the integer $n = 5$, meaning that within five continuous steps, the maximum relative error of the objective function has a higher tolerance.

3. Numerical examples and discussions

The commercial software ANSYS [57] which is connected with the self-developed MATLAB codes for design optimisation, is used for finite element analysis of structures.

3.1. Example 1

Fig. 1 shows the design domain, a rectangle plate (20 m * 10 m, thickness is 0.05 m) with the upper and right sides fixed. The whole design domain is discretised with 800 eight-nodal plane stress elements. For the artificial material model: The Young's modulus is 200 GPa, and Poisson's ratio is 0.3. The structure is subject to two uncertain loads: (1) The horizontal concentrated force is $P_1 \sim N(50 \text{ kN}, \sigma_{P_1}^2)$ applied at the centre of the bottom, and (2) The concentrated force is $P_2 \sim N(200 \text{ kN}, \sigma_{P_2}^2)$ applied vertically as the second load. The weighting coefficients are the same for each case ($w_1 = w_2 = 0.5$). The volume fraction is 15%. Both cases are considered under $\sigma_{P_1} = 2 \text{ kN}$, 5 kN and $\sigma_{P_2} = 2 \text{ kN}$.

Fig. 2 gives the optimal topologies of the structure in Fig. 1 under MLC. Fig. 2(a) is the deterministic design by SIMP [55]. The other two plots, Fig. 2(b) and (c), show the robust designs. The results are the same as those given by Luo et al. [17]. Therefore, the proposed method is valid to complete a robust design of isotropic material.

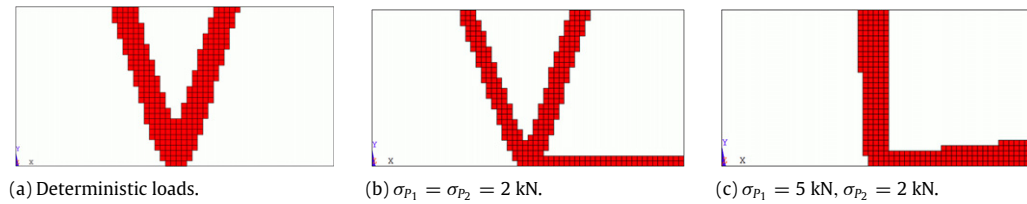


Fig. 2. Isotropic material optimal layouts under uncertain loads.

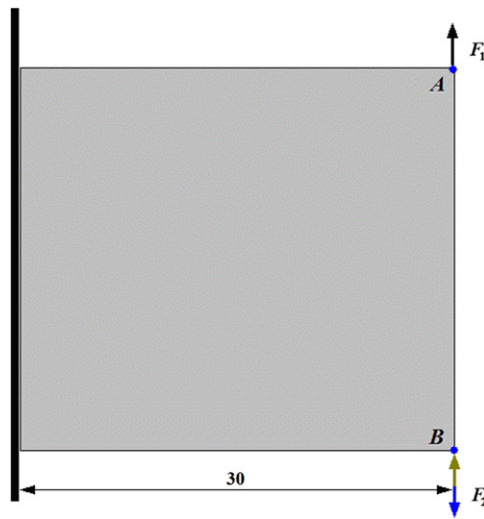


Fig. 3. The initial design domain under two uncertain loading cases.

3.2. Example 2

The design domain of the structure, with two vertical sides fixed, is shown in Fig. 3, which is a $l \times l$ ($l = 1.0$ m) square plate with a thickness of 0.01 m. The design domain is discretised with 2500 four-nodal plane stress elements, subject to two loading conditions. In the first case, the concentrated upward force $F_1 \sim N(1000 \text{ N}, 20^2)$ is applied at the centre of the top with a weighting coefficient w_1 . In the second case, the concentrated force $F_2 \sim N(1000 \text{ N}, \sigma_{F_2}^2)$ is applied at the bottom of the right side with the weight coefficient w_2 . The direction of F_2 is vertical but not determined to be upward (\uparrow) or downward (\downarrow). The tension modulus of material is 200 GPa, and its Poisson's ratio is 0.3. The material volume is constrained to 40%.

The following effects on the optimal material layouts are considered:

- (1) Different directions (\downarrow or \uparrow) of F_2 ;
- (2) Different values of standard deviation of F_2 , i.e., σ_{F_2} ;
- (3) Different values of R_{TCE} .

In the following discussions, (a) the isotropic material in the following cases means the structure with isotropic material (modulus 200 GPa and Poisson's ratio 0.3); (b) For bi-modulus material, the value R_{TCE} gives the difference between tension and compression moduli of the material; (c) Given that we do not consider the effects of weighting schemes on optimal topologies, the two weighting coefficients are equal in this numerical case, i.e., $w_1 = w_2 = 0.5$.

Fig. 4 shows the deterministic design of the structure under two loading cases. Based on Fig. 4(a) and (b), it can be seen that the two results are the same, indicating that the isotropic material layout is not sensitive to the loading directions. However, Fig. 4(c) and (d) show different material layouts, as the material in the design domain is bi-modulus. All four figures have one symmetric plane,

which may be the major difference that distinguishes them from the robust designs discussed in the following section.

3.2.1. The effects of F_2 directions on material layouts

In this section, the value of σ_{F_2} is set to 50 N. For purposes of comparison, the structures under deterministic loads or uncertain loads will be displayed.

Fig. 5 shows the robust design of materials in the structure. Fig. 5(a) and (b) show the optimal distributions of isotropic material under uncertain loads. The distributions are identical, implying that the isotropic material layout is not sensitive to the direction of F_2 . Fig. 5(c) and (d) show the bi-modulus material layouts under uncertain loads, which are clearly different. The material distributes differently on the left side of the structure; thus, it can be inferred that bi-modulus material layout is sensitive to the direction of F_2 .

3.2.2. The effects of SD (σ_{F_2}) on material layouts

The direction of F_2 is always downward in this section. For bi-modulus material, $R_{TCE} = 0.5$. The two weighting coefficients are equal, i.e., $w_1 = w_2 = 0.5$. Three numerical cases for structures with either isotropic material or bi-modulus material are given as follows: (I) $\sigma_{F_2} = 10$ N; (II) $\sigma_{F_2} = 20$ N; (III) $\sigma_{F_2} = 100$ N.

Fig. 6 gives the optimal material (isotropic or bi-modulus material) distributions under different uncertain loads. It can be seen that the material tends to support F_1 when $\sigma_{F_2} = 10$ N (less than $\sigma_{F_1} = 20$ N) (see Fig. 6(a) and (b)). For $\sigma_{F_1} = \sigma_{F_2} = 20$ N, the topologies are symmetric (see Fig. 6(c) and (d)). When $\sigma_{F_2} = 100$ is much greater than $\sigma_{F_1} = 20$, the amount of material required to support F_1 in the final structure is very low (see Fig. 6(e) and (f)). Therefore, the optimal layout of a structure under uncertain loads is determined using standard deviation values rather than directly by the values of forces.

3.2.3. The effects of R_{TCE} on material layouts

The direction of F_2 is always downward in this section. The two weighting coefficients are equal, i.e., $w_1 = w_2 = 0.5$. σ_{F_2} is 50 N. Two cases with bi-modulus materials in the structure are considered, e.g., (I) $R_{TCE} = 0.2$ vs. $R_{TCE} = 5$; (II) $R_{TCE} = 0.5$ vs. $R_{TCE} = 2$.

Fig. 7(a) displays the optimal layout for bi-modulus material ($R_{TCE} = 0.2$) and indicates that the tension modulus is far less than the compression modulus. Therefore, the material under compression (in the second loading case) is much greater than that in the final structure, as shown in Fig. 7(b)–(d). The differences between Fig. 7(a) and (b) and between Fig. 7(c) and (d) are clear. There is no symmetry between these topological plots. It can also be noted that as the value of R_{TCE} increases, the inner part of the final structure strengthens.

4. Conclusions

The effects of uncertainty are naturally a consideration for practical engineering design, especially for structures under uncertain

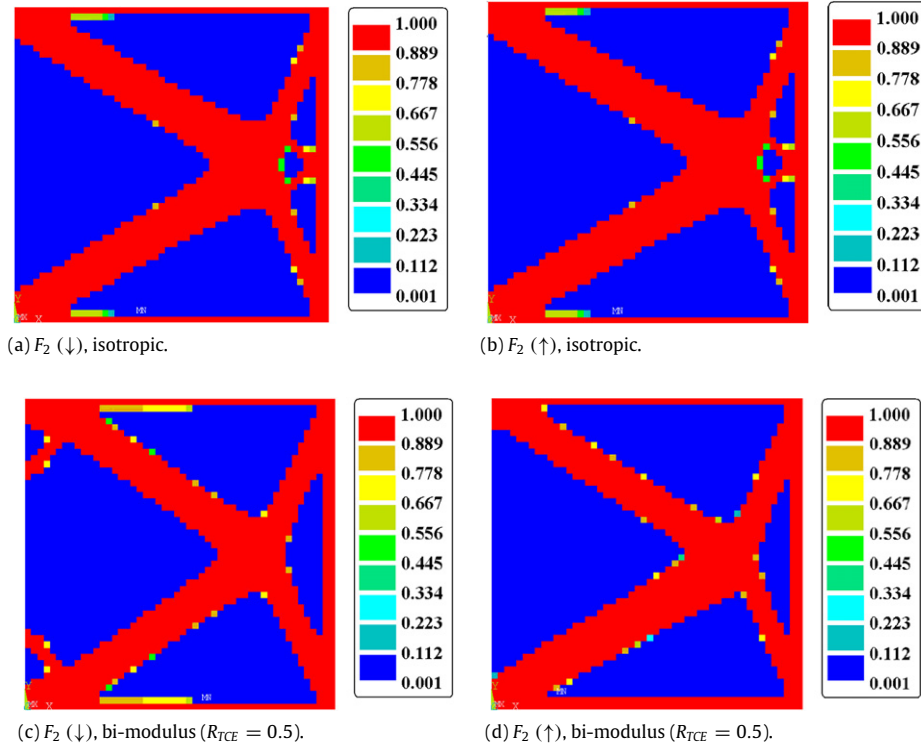


Fig. 4. Optimal material layouts under deterministic MLCs ($w_1 = w_2 = 0.5$).

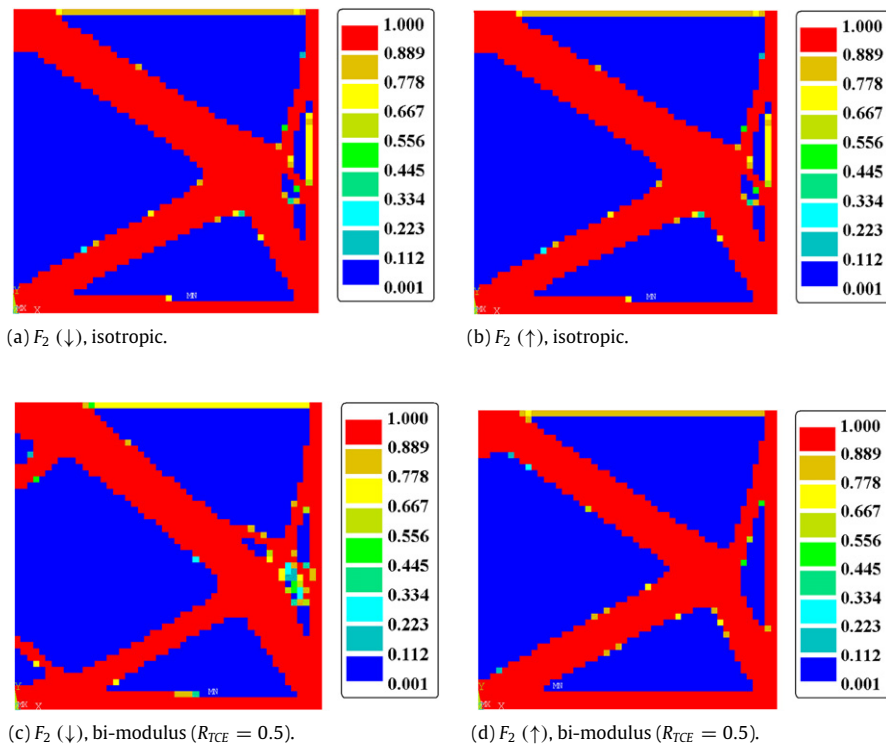


Fig. 5. Optimal material layouts under uncertain MLCs.

multiple loading conditions. Based on material replacement operation, a sensitivity analysis for the topology optimisation of bi-modulus structures is implemented in this study. Numerical examples are given to discuss the effects of various parameters on the final material distributions. These parameters include force

directions, weighting schemes of loads, standard deviations and the difference between two moduli of a bi-modulus material. From the numerical results, we can assert the following conclusions:

(1) Under either deterministic loads or uncertain loads, the final layout of bi-modulus material is sensitive to force directions (i.e.,

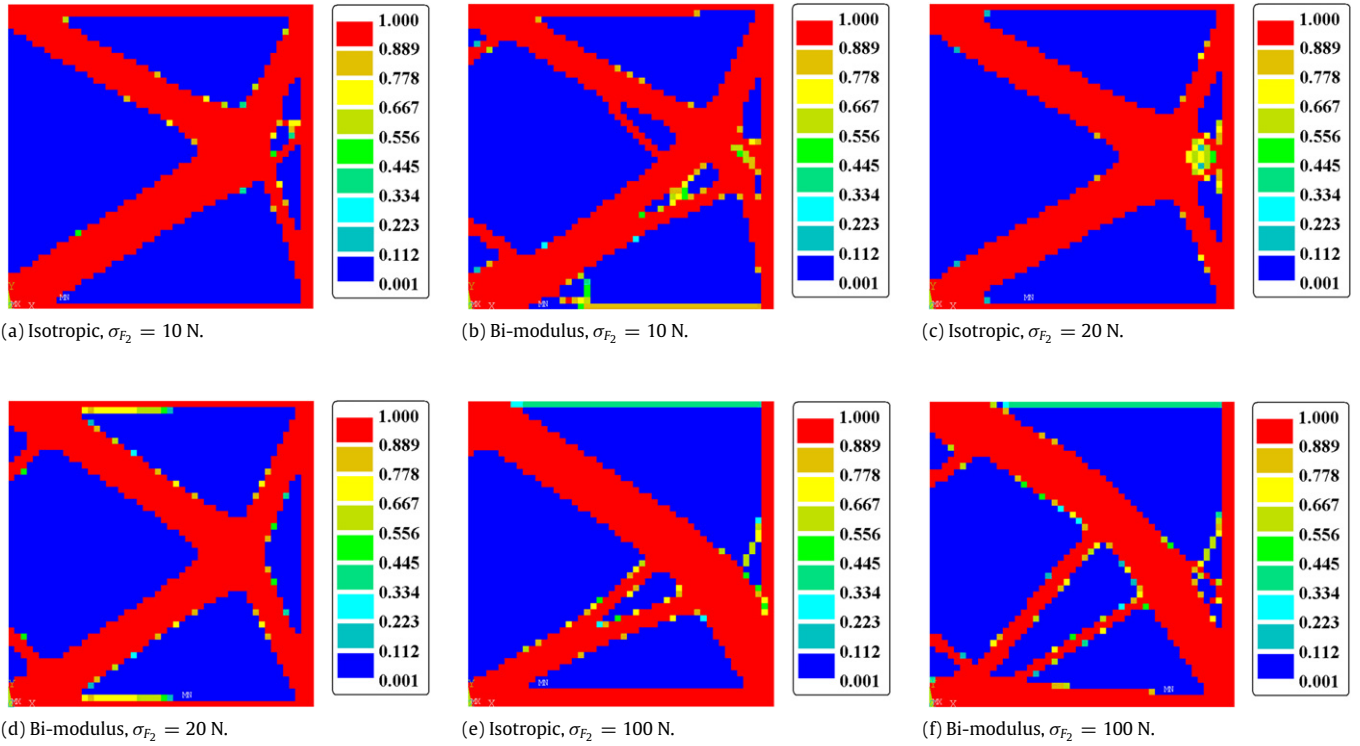


Fig. 6. Optimal material layouts under various uncertain loads.

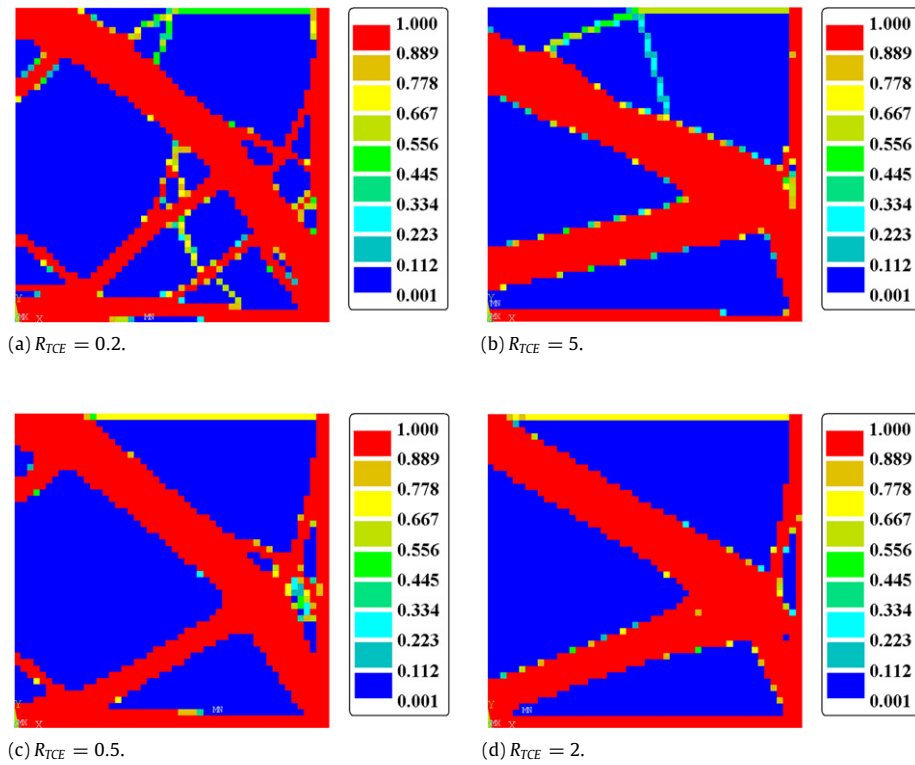


Fig. 7. Optimal bi-modulus material layouts under uncertain loads.

F v.s. **−F**), which is compared to isotropic material layouts, which are not sensitive to force directions; (2) The values of the standard deviations of uncertain forces rather than the forces themselves influence the final material distributions; (3) The effects of the

two moduli of a bi-modulus material on the final optimal design are clear. In the final structure, the amount of material that absorbs greater strain energy will be implemented as much as possible.

Acknowledgements

Financial support from the National Natural-Science-Foundation of China (50908190, 51279171), the Youth Talents Foundation of Shanxi Province (2011KJXX02), and Research Foundation (GZ1205) of State Key Laboratory of Structural Analysis for Industrial Equipment, Dalian University of Technology, Dalian 116024, PR China are greatly acknowledged.

References

- [1] Bendsøe MP, Sigmund O. Topology optimization: theory, methods, and applications. Berlin, Heidelberg: Springer; 2003.
- [2] Bendsøe MP, Ben-Tal A, Zowe J. Optimization methods for truss geometry and topology design. Optimal design of material properties and material distribution for multiple loading condition. *Structural and Multidisciplinary Optimization* 1994;7:197–224.
- [3] Bendsøe MP, Kikuchi N. Generating optimal topologies in structural design using a homogenization method. *Computer Methods in Applied Mechanics and Engineering* 1988;71:197–224.
- [4] Zhou M, Rozvany GN. The COC algorithm, part II: topological, geometry and generalized shape optimization. *Computer Methods in Applied Mechanics and Engineering* 1991;89:197–224.
- [5] Qin QH, He XQ. Variational principles, FE and MPT for analysis of nonlinear impact contact problems. *Computer Methods in Applied Mechanics and Engineering* 2005;122:205–22.
- [6] Xie YM, Steven GP. A simple evolutionary procedure for structural optimization. *Computers and Structures* 1993;49(5):885–96.
- [7] Guan H, Steven GP, Xie YM. Evolutionary structural optimization incorporating tension and compression materials. *Advances in Structural Engineering* 1999;2(4):273–88.
- [8] Alfieri L, Bassi D, Biondini F, Malerba PG. Morphologic evolutionary structural optimization. In: Proc. 7th world congress on structural and multidisciplinary optimization, paper A0422. 2007.
- [9] Wang MY, Wang X, Guo D. A level set method for structural topology optimization. *Computer Methods in Applied Mechanics and Engineering* 2003;192(1):227–46.
- [10] Allaire G, Jouve F, Toader AM. Structural optimization using sensitivity analysis and a level-set method. *Journal of Computational Physics* 2004;194:363–93.
- [11] Luo Z, Tong L, Kang Z. A level set method for structural shape and topology optimization using radial basis functions. *Computers and Structures* 2009;87(7):425–34.
- [12] Schuëller GI, Jenson HA. Computational methods in optimization considering uncertainties—an overview. *Computer Methods in Applied Mechanics and Engineering* 2008;198(1):2–13.
- [13] Papadrakakis M, Lagaros ND. Reliability-based structural optimization using neural networks and Monte Carlo simulation. *Computer Methods in Applied Mechanics and Engineering* 2002;191(32):3491–507.
- [14] Valdebenito MA, Schuëller GI. A survey on approaches for reliability-based optimization. *Structural and Multidisciplinary Optimization* 2010;42(5):645–63.
- [15] Doltsinis I, Kang Z. Robust design of structures using optimization methods. *Computer Methods in Applied Mechanics and Engineering* 2004;193(23–26):2221–37.
- [16] Beyer HG, Sendhoff B. Robust optimization—a comprehensive introduction. *Computer Methods in Applied Mechanics and Engineering* 2007;196(33–34):3190–218.
- [17] Luo Y, Kang Z, Deng Z. Robust topology optimization of structures with multiple load cases. *Chinese Journal of Theoretical and Applied Mechanics* 2011;43(1):227–34.
- [18] Kharmanda G, Olhoff N. Reliability-based topology optimization as a new strategy to generate different structural topologies. In: 15th Nordic seminar on computational mechanics. 2002.
- [19] Kharmanda G, Olhoff N, Mohamed A, Lemaire M. Reliability-based topology optimization. *Structural and Multidisciplinary Optimization* 2004;26(5):295–307.
- [20] Maute K, Frangopol DM. Reliability-based design of MEMS mechanisms by topology optimization. *Computers and Structures* 2003;81(8–11):813–24.
- [21] Allen M, Maute K. Reliability-based shape optimization of structures undergoing fluid–structure interaction phenomena. *Computer Methods in Applied Mechanics and Engineering* 2005;194(30–33):3472–95.
- [22] Kim SR, Park JY, Lee WG, Yu JS, Han SY. Reliability-based topology optimization based on evolutionary structural optimization. *International Journal of Mechanical Systems Science and Engineering* 2008;1(3):135–9.
- [23] Jung HS, Cho S. Reliability-based topology optimization of geometrically nonlinear structures with loading and material uncertainties. *Finite Elements in Analysis and Design* 2004;41(3):311–31.
- [24] Luo Y, Kang Z, Luo Z, Li A. Continuum topology optimization with non-probabilistic reliability constraints based on multi-ellipsoid convex model. *Structural and Multidisciplinary Optimization* 2009;39(3):297–310.
- [25] Guest JK, Igusa T. Structural optimization under uncertain loads and nodal locations. *Computer Methods in Applied Mechanics and Engineering* 2008;198(1):116–24.
- [26] Silva M, Tortorelli DA, Norato JA, Ha C, Bae HR. Component and system reliability-based topology optimization using a single-loop method. *Structural and Multidisciplinary Optimization* 2010;41(1):87–106.
- [27] Nguyen TH, Song J, Paulino GH. Single-loop system reliability-based topology optimization considering statistical dependence between limit-states. *Structural and Multidisciplinary Optimization* 2011;44(5):593–611.
- [28] Kang Z, Luo Y. Non-probabilistic reliability-based topology optimization of geometrically nonlinear structures using convex models. *Computer Methods in Applied Mechanics and Engineering* 2009;198(41–44):3228–38.
- [29] Chen S, Chen W, Lee S. Level set based robust shape and topology optimization under random field uncertainties. *Structural and Multidisciplinary Optimization* 2010;41(1):507–24.
- [30] Kogiso N, Ahn W, Nishiwaki S, Izui K, Yoshimura M. Robust topology optimization for compliant mechanisms considering uncertainty of applied loads. *Journal of Advanced Mechanical Design, Systems, and Manufacturing* 2008;2(1):96–107.
- [31] Seepersad CC, Alien JK, McDowell DL, Mistree F. Robust design of cellular materials with topological and dimensional imperfections. *ASME Journal of Mechanical Design* 2006;128:1285–97.
- [32] Luo Z, Chen L, Yang J, Zhang Y, Abdel-Malek K. Fuzzy tolerance multilevel approach for structural topology optimization. *Computers and Structures* 2006;84(3):127–40.
- [33] Ambartsumyan SA. Equations of the theory of thermal stresses in double-modulus materials. In: Proc. IUTAM symposium. East Kilbride-Vienna and New York: Springer-Verlag; 1970.
- [34] Medri G. A nonlinear elastic model for isotropic materials with different behavior in tension and compression. *Transactions of the ASME—Journal of Engineering Materials* 1982;104(1):26–8.
- [35] Jung D, Gea HC. Topology optimization of nonlinear structures. *Finite Elements in Analysis and Design* 2004;40(11):1417–27.
- [36] Desmorat B, Duvaut G. Compliance optimization with nonlinear elastic materials application to constitutive laws dissymmetric in tension–compression. *European Journal of Mechanics, A/Solids* 2003;22(2):179–92.
- [37] Chang CJ, Zheng B, Gea HC. Topology optimization for tension/compression only design. In: Proc. 7th world congress on structural and multidisciplinary optimization. COEX. 2007. p. 2488–95.
- [38] Cai K, Shi J. A heuristic approach to solve stiffness design of continuum structures with tension/compression-only materials. In: Proc. 4th international conference on natural computation, vol. 1. 2008. p. 131–5.
- [39] Querin OM, Victoria M, Marti P. Topology optimization of truss-like continua with different material properties in tension and compression. *Structural and Multidisciplinary Optimization* 2010;42(1):25–32.
- [40] Liu ST, Qiao HT. Topology optimization of continuum structures with different tensile and compressive properties in bridge layout design. *Structural and Multidisciplinary Optimization* 2011;43(3):369–80.
- [41] Cai K. A simple approach to find optimal topology of a continuum with tension-only or compression-only material. *Structural and Multidisciplinary Optimization* 2011;43(6):827–35.
- [42] Duysinx P. Topology optimization with different stress limit in tension and compression. In: Third world congress of structural and multidisciplinary optimization, WCSMO3. 1999.
- [43] Bruggi M, Duysinx P. Topology optimization for minimum weight with compliance and stress constraints. *Structural and Multidisciplinary Optimization* 2012;46:369–84.
- [44] Luo Y, Kang Z. Topology optimization of continuum structures with Drucker–Prager yield stress constraints. *Computers and Structures* 2012;90–91:65–75.
- [45] Jeong SH, Park SH, Choi DH, Yoon GH. Topology optimization considering static failure theories for ductile and brittle materials. *Computers and Structures* 2012;110–111:116–32.
- [46] Díaz AR, Bendsøe MP. Shape optimization of structures for multiple loading condition using a homogenization method. *Structural and Multidisciplinary Optimization* 1992;4:17–22.
- [47] Bendsøe MP, Diaz AR, Taylor EJ. Optimal design of material properties and material distribution for multiple loading condition. *International Journal for Numerical Methods in Engineering* 1995;38(7):1149–70.
- [48] Sui YK, Yang DQ, Wang B. Topological optimization of continuum structure with stress and displacement constraints under multiple loading cases. *Chinese Journal of Theoretical and Applied Mechanics* 2000;32(2):171–9.
- [49] Cheng GD, Zheng J. Study on topology optimization with stress constraints. *Engineering Optimization* 1992;20:129–48.
- [50] Duysinx P, Bendsøe MP. Topology optimization of continuum structures with local stress constraints. *International Journal for Numerical Methods in Engineering* 1998;43:1453–78.
- [51] Qin QH. Trefftz finite element method and its applications. *Applied Mechanics Reviews* 2005;58:316–37.
- [52] Qin QH, Wang H. Matlab and C programming for Trefftz finite element methods. Boca Raton: Taylor & Francis; 2008.
- [53] Taguchi G. Taguchi on robust technology development: bringing quality engineering upstream. New York: ASME Press; 1993.

- [54] Rosenblatt M. Remarks on a multivariate transformation. *Annals of Mathematical Statistics* 1952;23(3):470–2.
- [55] Sigmund O. A 99 line topology optimization code written in Matlab. *Structural Multidisciplinary Optimization* 2001;21(2):120–7.
- [56] Bruns TE, Tortorelli DA. Topology optimization of non-linear elastic structures and compliant mechanisms. *Computer Methods in Applied Mechanics and Engineering* 2001;190:3443–59.
- [57] Ansys Inc., ANSYS. 2012. <http://www.ansys.com>.